RAPID COMMUNICATIONS

PHYSICAL REVIEW E VOLUME 49, NUMBER 4 APRIL 1994

Experimental control of chaos by means of weak parametric perturbations

R. Meucci, W. Gadomski,* M. Ciofini, and F. T. Arecchi
Istituto Nazionale di Ottica, 50125 Firenze, Italy
(Received 20 December 1993)

The dynamical regime of a single mode laser with modulated losses in the chaotic parameter range has been stabilized over one of the periodic orbits contained within the strange attractor by controlling the phase of a small periodic perturbation of the forcing term. Numerical solutions of a theoretical model show a good agreement with the experiment and provide the size of the stability windows in the parameter space.

PACS number(s): 05.45.+b, 42.50.Lc, 42.55.Lt

Controlling chaos represents one of the most interesting and challenging programs in the field of nonlinear dynamics. The basic idea is to stabilize the dynamics over one of the different periods visited during the chaotic motion by applying only small perturbations to the system. This makes it advantageous to deal with chaotic attractors, since they contain an infinite number of different unstable orbits [1,2] and hence provide a large choice at a low cost, i.e., by a small perturbation. On the other hand, in many situations one may wish to avoid or reduce undesired chaotic instabilities by the help of small perturbations, without introducing radical changes in the experimental configuration.

In the past few years different methods have been proposed based (i) on the determination of the stable and unstable directions in the Poincaré section [3–6], (ii) on a self-controlling feedback procedure [7], and (iii) on the introduction of small perturbations [8–12]. As for case (iii), theoretical works have dealt with the suppression of chaos in the dynamics of a Duffing-Holmes oscillator [8,9]. In Ref. [8] the perturbation consists of a parametric modulation of the cubic term, while Ref. [9] introduces an additive anharmonic forcing term. The presence of a weak periodic external forcing has been demonstrated to reduce chaotic instabilities also in the case of a periodically driven pendulum [10]. From an experimental point of view, it has been shown that small periodic perturbations allow control of chaos in a microwave-pumped spin wave instability [11], as well as in a bistable magnetoelastic system [12]. Although the validity in the general case has been rigorously proved only for method (i), methods (ii) and (iii) look more suitable for experimental situations, because they do not require a real-time computer analysis of the state of the system and they seem more robust to noise.

In this paper we show how a small parametric perturbation stabilizes the chaotic behavior of a CO_2 laser with modulated losses. Provided there is a suitable phase difference between the fundamental signal which modulates the losses and the perturbation, robust stabilization of different periodic orbits can be achieved with perturbation amplitudes of a few percent. Numerical simulations of an improved four-level model [13,14] for the CO_2 laser confirm the experimental results with a good degree of accuracy.

The experimental apparatus consists of a single mode CO_2 laser with an intracavity electro-optic modulator (EOM) allowing modulation of the cavity losses. The optical cavity is 1.35 m long and the total transmission coefficient T is 0.10 for a single pass. The intensity decay rate $k(t)$ can be expressed as follows [14]:

$$k(t) = \frac{c}{2L}\{2T + (1-2T)\sin^2[\pi V(t)/V_\lambda]\}, \qquad (1)$$

where $V_\lambda = 4240$ V and $V(t)$ is the voltage applied to the modulator,

$$V(t) = V_0 + V_1 A \sin(2\pi F t), \qquad (2)$$

with $V_0 = 600$ V, $F = 100$ kHz, and $A = 70$ is an amplification factor. It is well known that, by increasing the amplitude modulation V_1, the system undergoes a subharmonic sequence of bifurcations leading to chaos [15]. We have studied the bifurcation diagram by recording the values of V_1 for which successive bifurcations occur. We have found that $F/2$ appears for $V_1 = 0.5$ V, $F/4$ for $V_1 = 1.05$ V, $F/8$ for $V_1 = 1.20$ V, and a wide chaotic window is present between $V_1 = 1.22$ V and $V_1 = 1.75$ V bounded by the $F/3$ period window.

The stabilization of periodic orbits within the chaotic region has been obtained by slight modulations of the control parameter V_1. Such perturbations consist of sinusoidal signals at $f = f_1 = 50$ kHz and $f = f_2 = 25$ kHz with amplitude ε and an adjustable phase offset $\alpha = m\pi$ with respect to the fundamental signal $V(t)$, that is,

$$V_1(t) = V_1[1 + \varepsilon \sin(2\pi f_i t + \alpha)], \quad i = 1, 2. \qquad (3)$$

An electronic loop allows a linear sweep of the phase term α of π radians. The modulation circuit is sketched in Fig. 1. A Tektronix arbitrary function generator (AFG) is set to a sinusoidal output signal of frequency 100 kHz and amplitude V_1. The reference output of the AFG drives a frequency divider (FD) which triggers a sawtooth signal. The sawtooth signal, added to a triangular signal of 0.1 Hz, acts as the trigger of the function generator (FG) which feeds back the amplitude-

*Permanent address: Department of Chemistry, University of Warsaw, 02-089 Warsaw, Poland.

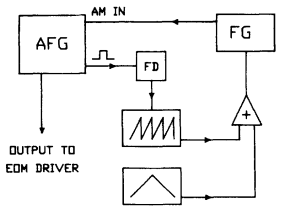

FIG. 1. Schematic diagram of the electronic circuitry which allows linear sweeping of the parameter m.

modulation input of the AFG. In this way, a variable delay is generated between the fundamental signal from the AFG (frequency F) and the modulating signal from the FG (frequency f_i), because each trigger event of the FG occurs for a different voltage level of the sawtooth, due to the triangular wave. In the case of 25 kHz perturbation, the divider is replaced by a divider by four.

The experimental results are shown in Figs. 2–5 for 50 and 25 kHz. In Fig. 2 we report a stroboscopic recording (sampling period $1/F$, scanning time 5 sec) of the laser intensity I versus the parameter m, for $V_1 = 1.3$ V and $\varepsilon = 0.025$. The laser behavior in the range $0.6 < m < 1.6$ is completely symmetric with respect to that reported in Fig. 2. It is clear that, by choosing a suitable phase, it is possible to stabilize periodic orbits embedded in the chaotic attractor. Once the appropriate phase is selected, the stability is of the order of several minutes, until uncontrolled drifts spoil the resonance condition between the cavity mode and the gain line. In Fig. 3 we show Poincaré sections for $m = -0.2$ and $m = 0.6$ (same parameter values as Fig. 2) constructed by plotting I_{n+1} vs I_n, where $I_n = I(t = n/F)$. Figure 4 shows the results obtained at 25 kHz for $V_1 = 1.4$ V and $\varepsilon = 0.03$. Symmetric behavior is obtained for $1.0 < m < 2.0$. The two Poincaré sections in the periodic ($m = 0.0$) and in the chaotic ($m = 0.4$) regimes, with the same parameter values as Fig. 4, are reported in Fig. 5. In both cases of 50 and 25 kHz perturbations, stabilization can be obtained within the chaotic window with perturbation amplitudes $\varepsilon < 0.08$.

As we aim at a quantitative fit between a theoretical

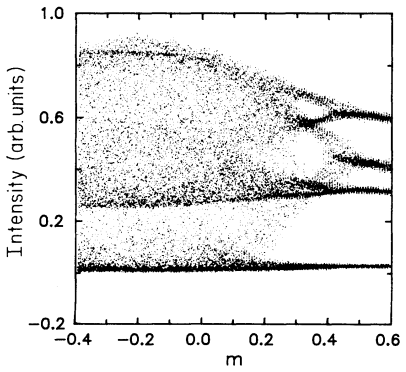

FIG. 2. Experimental results with 2.5% perturbation at $F/2$. Stroboscopic recording of the laser intensity (arbitrary units) versus the relative phase offset m of the perturbation with respect to the main modulation signal.

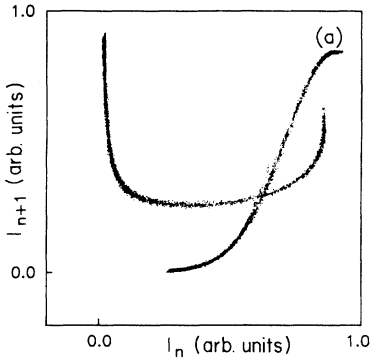

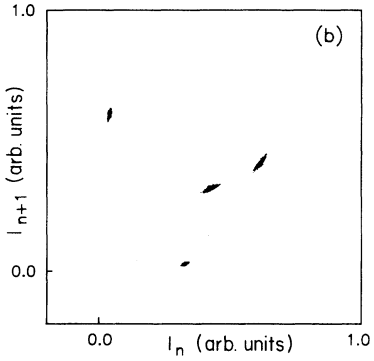

FIG. 3. Return maps of the normalized output intensity I with the parameters of Fig. 2 for two phase offsets: (a) $m = -0.2$, (b) $m = 0.6$.

model and the experiment, the two-level model used in the first reports on chaos in a CO_2 laser [15] are not sufficient, since the chaotic dynamics, as well as its control, occur on a time range longer than the collisional coupling of the resonant transition with the other energy levels within the same vibrational state. A more detailed model accounting for the coupling between the two laser levels and their rotational manifolds is required, as discussed in Refs. [13,14] where a four-level model (4LM) provides quantitative agreement with the experimental data in chaotic dynamics. The 4LM consists of five differential equations for the intensity I, the populations N_2 and N_1 of the upper and lower lasing states, and the

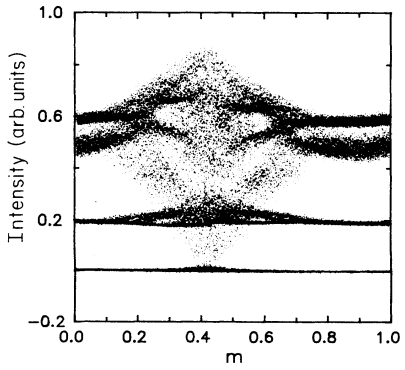

FIG. 4. Experimental stroboscopic data of the laser intensity with 3.0% perturbation at $F/4$.

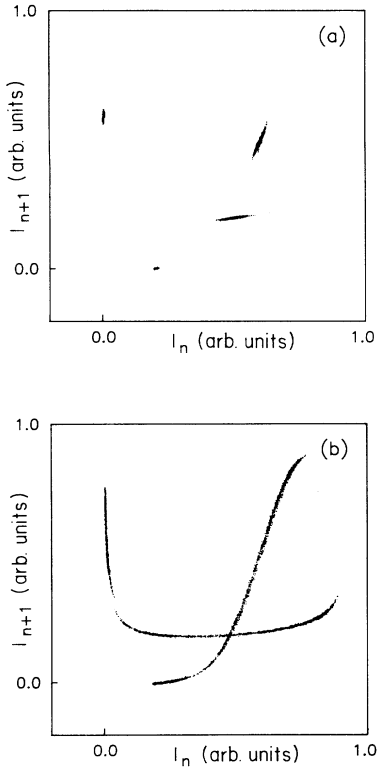

FIG. 5. Return maps of the output intensity I with the parameters of Fig. 4 for two phase offsets: (a) $m = 0.0$, (b) $m = 0.4$.

global populations M_2 and M_1 of the two manifolds of rotational levels which are coupled by collisions with N_2 and N_1 respectively:

$$\begin{aligned}
\dot{I} &= -k(t)I + G(N_2 - N_1)I, \\
\dot{N}_2 &= -(Z\gamma_R + \gamma_2)N_2 - G(N_2 - N_1)I + \gamma_R M_2 + \gamma_2 P, \\
\dot{N}_1 &= -(Z\gamma_R + \gamma_1)N_1 + G(N_2 - N_1)I + \gamma_R M_1, \qquad (4) \\
\dot{M}_2 &= -(\gamma_R + \gamma_2)M_2 + Z\gamma_R N_2 + Z\gamma_2 P, \\
\dot{M}_1 &= -(\gamma_R + \gamma_1)M_1 + Z\gamma_R N_1,
\end{aligned}$$

where $\gamma_R = 7.0 \times 10^5$ sec^{-1} is the relaxation rate between the lasing states and the associated rotational manifolds (the enhancement factor $Z = 10$ represents the number of sublevels considered in each manifold), and $\gamma_2 = 1.0 \times 10^4$ sec^{-1} and $\gamma_1 = 8.0 \times 10^4$ sec^{-1} are the relaxation rates of the vibrational states. Moreover, $G = 6.2 \times 10^{-8}$ sec^{-1} is the field-matter coupling constant, while the adimensional parameter $P = 6.35 \times 10^{14}$ represents the pump. The numerical values of the parameters are rescaled by following Ref. [14]. Using this set of parameter values we reproduce the bifurcation measurements with a good degree of accuracy, obtaining the sequence of bifurcations for values of V_1 which are at most 5% different from the experimental ones.

We have performed simulations modulating the control voltage V_1 according to Eq. (3). The agreement of the model with the experiment can be inferred from Fig. 6.

Figure 6(a) shows the stroboscopic recording of the laser intensity versus the parameter m, with a perturbation of 50 kHz frequency, $V_1 = 1.30$ V and $\varepsilon = 0.04$, while Fig. 6(b) represents the corresponding stroboscopic map obtained at fixed $m = -0.2$. The experimental features observed in the case of 25 kHz perturbation (Figs. 4 and 5) can be numerically reproduced with the same degree of accuracy using $V_1 = 1.35$ V and $\varepsilon = 0.04$.

The stabilization robustness can also be tested with respect to small changes of the perturbation frequency f around the resonant value $f_1 = 50$ kHz, keeping all the other parameters fixed. Let us introduce the phase difference $\Phi(t)$ between the fundamental signal (frequency F) and the perturbation signal (frequency $f = F/2 + \Delta f$). This can be expressed as

$$\begin{aligned}
\Phi(t) &= \pi F t - \alpha(t), \\
\alpha(t) &= (2\pi\, \Delta f\, t + m\pi).
\end{aligned}$$

The term $2\pi\, \Delta f\, t$ acts as a slowly varying modulation of the phase offset $\alpha(t)$ which, in the resonant case, reduces to $m\pi$. Thus the introduction of the detuning Δf is equivalent to a time dependent phase offset, so that the temporal evolution of the system consists of a regular alternation between stable orbits and chaotic behaviors.

In order to characterize the control procedure with respect to the parameter ε, let us define ε_{10} (ε_{50}) as the value for which we obtain stabilization within a relative

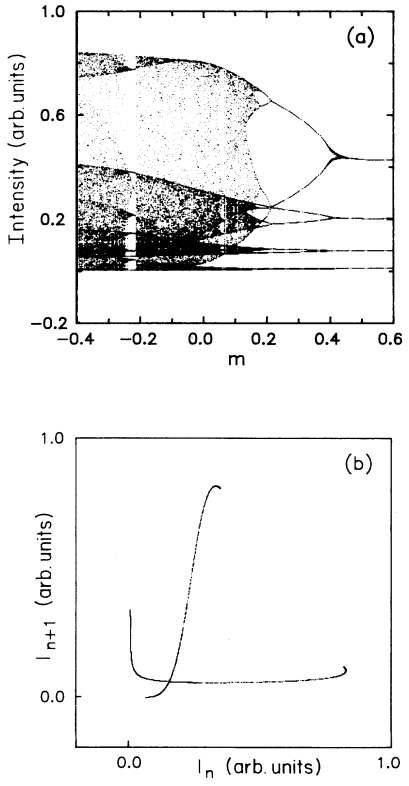

FIG. 6. Numerical simulations with 50 kHz perturbation, $V_1 = 1.3$ V and $\varepsilon = 0.04$; (a) stroboscopic recording of the intensity versus the relative phase offset m, (b) return map of the intensity at fixed $m = -0.2$.

phase interval $\Delta\alpha/2\pi = 0.10$ (0.50). The theoretical behavior of ε_{10} (solid line) and ε_{50} (dashed line) as a function of V_1 is reported in Fig. 7, together with the experimentally measured values of ε_{10}. Above $V_1 = 1.40$ V, there is no agreement between the experimental and theoretical ε_{10}. This implies that for large modulation strengths V_1, the model described by Eqs. (1)–(4) is no longer sufficient to predict the size of the stability window. More complex phenomena, possibly related to the detailed structure of the rotational levels, may play a role in fixing this parameter, even though simulations of the time series do not show appreciable differences from the experiment.

In summary, robust stabilization of the unstable orbits embedded in a chaotic attractor has been experimentally demonstrated for a single mode CO_2 laser with modulated losses. The stabilization is obtained by means of sinusoidal parametric perturbations having relative amplitudes of few percent and frequencies which are in ratios 1:2 and 1:4 with respect to the fundamental forcing frequency. In the case of chaos induced by an external sinusoidal forcing, stabilization by resonant perturbations at subharmonic frequencies of the main modulation was already discussed by several investigators [8–12]. A crucial problem of this type of stabilization is its robustness, that is, the size of the parameter window over which stabilization is achieved. The most reliable laboratory implementation is obtained by fixing the perturbation frequencies at the appropriate ratios of the main frequency and then scanning the phase offset $\alpha = m\pi$, as reported here. Since different values of the parameter m imply different initial conditions for the whole flow described in Eqs. (4), our analysis corresponds to the investigation of the size of the basins of attraction of the stabilized orbits.

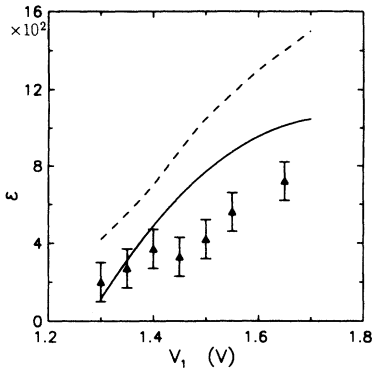

FIG. 7. Structural stability of the control method. Scaling of the perturbation amplitude ε which provides a relative stability window of 10% (solid line) and 50% (dashed line) of the whole phase domain 0–2π versus the modulation voltage V_1. Triangles denote the experimental measurements of the 10% window, with associated error bars.

This work was partly supported by the E. C. Contract No. SCI*-CT91-0697 (TSTS). One of us (W.G.) has been partly supported by the BW 945/26 Programme (University of Warsaw).

[1] D. Auerbach, P. Cvitanovic, J. P. Eckmann, G. Gunaratne, and I. Procaccia, Phys. Rev. Lett. **58**, 2387 (1987).

[2] C. Grebogi, E. Ott, and J. A. Yorke, Phys. Rev. A **37**, 1711 (1988).

[3] E. Ott, C. Grebogi, and J. A. Yorke, Phys. Rev. Lett. **64**, 1196 (1990); W. L. Ditto, S. N. Rauseo, and M. L. Spano, *ibid.* **65**, 3211 (1990); U. Dressler and G. Nitsche, *ibid.* **68**, 1 (1992).

[4] B. Peng, V. Petrov, and K. Showalter, J. Phys. Chem. **95**, 4957 (1991).

[5] P. Parmananda, P. Sherard, R. W. Rollins, and H. D. Dewald, Phys. Rev. E **47**, R3003 (1993).

[6] E. R. Hunt, Phys. Rev. Lett. **67**, 1953 (1991); R. Roy, T. W. Murphy, T. D. Maier, Z. Gills, and E. R. Hunt, *ibid.* **68**, 1259 (1992).

[7] K. Pyragas, Phys. Lett. A **170**, 421 (1992); K. Pyragas and A. Tamaševicius, *ibid.* **180**, 99 (1993).

[8] R. Lima and M. Pettini, Phys. Rev. A **41**, 726 (1990).

[9] R. Chacón and J. Díaz Bejarano, Phys. Rev. Lett. **71**, 3103 (1993).

[10] Y. Braiman and I. Goldhirsch, Phys. Rev. Lett. **66**, 2545 (1991).

[11] A. Azevedo and S. M. Rezende, Phys. Rev. Lett. **66**, 1342 (1991).

[12] L. Fronzoni, M. Giocondo, and M. Pettini, Phys. Rev. A **43**, 6483 (1991).

[13] J. Duprè, F. Meyer, and C. Meyer, Rev. Phys. Appl. **10**, 285 (1975); E. Arimondo, F. Casagrande, L. A. Lugiato, and P. Glorieux, Appl. Phys. B **30**, 57 (1983).

[14] R. Meucci, M. Ciofini, and Peng-ye Wang, Opt. Commun. **91**, 444 (1992); M. Ciofini, A. Politi, and R. Meucci, Phys. Rev. A **48**, 605 (1993); C. L. Pando L., R. Meucci, M. Ciofini, and F. T. Arecchi, Chaos **3**, 279 (1993).

[15] F. T. Arecchi, R. Meucci, G. P. Puccioni, and J. R. Tredicce, Phys. Rev. Lett. **49**, 1217 (1982); G. P. Puccioni, A. Poggi, W. Gadomski, J. R. Tredicce, and F. T. Arecchi, *ibid.* **55**, 339 (1985).

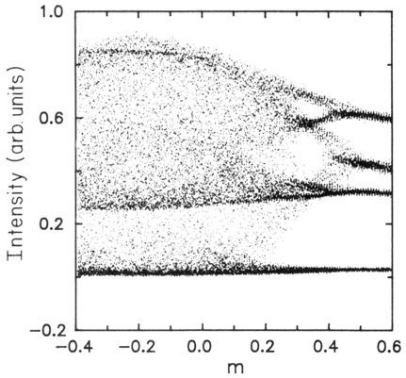

FIG. 2. Experimental results with 2.5% perturbation at $F/2$. Stroboscopic recording of the laser intensity (arbitrary units) versus the relative phase offset m of the perturbation with respect to the main modulation signal.

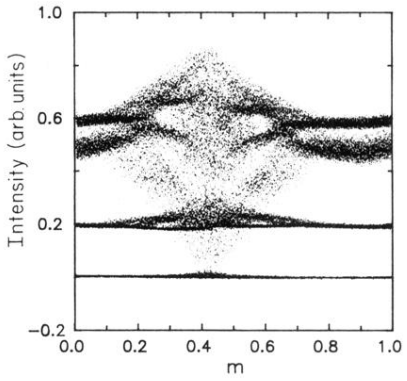

FIG. 4. Experimental stroboscopic data of the laser intensity with 3.0% perturbation at $F/4$.

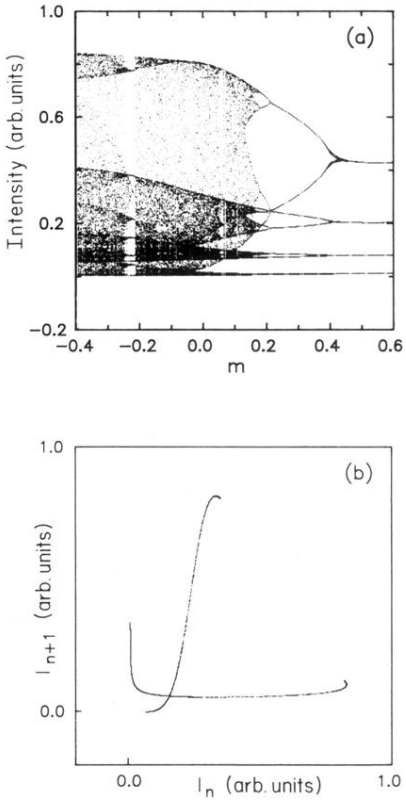

FIG. 6. Numerical simulations with 50 kHz perturbation, $V_1 = 1.3$ V and $\varepsilon = 0.04$; (a) stroboscopic recording of the intensity versus the relative phase offset m, (b) return map of the intensity at fixed $m = -0.2$.